



## Antinociceptive effect of isoorientin against neuropathic pain induced by the chronic constriction injury of the sciatic nerve in mice

Guoxin Zhang<sup>a,1</sup>, Ning Liu<sup>a,b,1</sup>, Chunhao Zhu<sup>a</sup>, Lin Ma<sup>c</sup>, Jiamei Yang<sup>a,b</sup>, Juan Du<sup>a</sup>,  
Wenjin Zhang<sup>a,b</sup>, Tao Sun<sup>c</sup>, Jianguo Niu<sup>c,\*</sup>, Jianqiang Yu<sup>a,b,c,\*\*</sup>

<sup>a</sup> Department of Pharmacology, College of Pharmacy, Ningxia Medical University, Yinchuan 750004, PR China

<sup>b</sup> Ningxia Hui Medicine Modern Engineering Research Center and Collaborative Innovation Center, Ningxia Medical University, Yinchuan 750004, PR China

<sup>c</sup> Ningxia Key Laboratory of Craniocerebral Diseases of Ningxia Hui Autonomous Region, Ningxia Medical University, Yinchuan 750004, PR China

### ARTICLE INFO

#### Keywords:

Isoorientin  
Neuropathic pain  
Antinociceptive  
Oxidative stress  
Matrix metalloproteinase-9  
Neuroinflammation

### ABSTRACT

Neuropathic pain is a widespread and debilitating chronic pain and the treatment remains a clinical challenge. Isoorientin (3',4',5,7-tetrahydroxy-6-C-glucopyranosyl flavone) is a natural flavonoid-like compound that exhibits antioxidant and anti-inflammatory activities; however, its effect on neuropathic pain remains unclear. Our study aimed to evaluate the antinociceptive effect of isoorientin in neuropathic pain mouse models induced by chronic constriction injury (CCI). In our study, the mice with CCI were administered with 7.5, 15, and, 30 mg/kg isoorientin for 8 consecutive days. Behavioral parameters were assayed on days 0, 7, 8, 10, 12, and 14 post-CCI surgery. Electrophysiological, histopathological, and biochemical indices were analyzed on day 14. Immunofluorescence was utilized to examine matrix metalloproteinase-9 (MMP-9) and glial cell activation, and proinflammatory cytokine expression levels were detected via Western blot. It is obvious that the treatment of Isoorientin remarkably ameliorated hyperalgesia and allodynia, increased sensory nerve conduction velocities, and restored CCI-induced sciatic nerve damage in mice. Isoorientin treatment significantly increased the total antioxidant capacity (T-AOC), total superoxide dismutase (T-SOD) and catalase (CAT) levels, and decreased the malondialdehyde (MDA) concentrations. Isoorientin also suppressed MMP-9 and glial cell activation, and downregulated tumor necrosis factor- $\alpha$  (TNF- $\alpha$ ), interleukin-6 (IL-6) and interleukin-1 $\beta$  (IL-1 $\beta$ ) expression levels. Therefore, this study provided a novel approach for neuropathic pain treatment and new insights into the pharmacological action of isoorientin.

### 1. Introduction

Neuropathic pain is due to somatosensory nervous system lesion or dysfunction and commonly accompanied with allodynia and hyperalgesia [1,2]. Epidemiological surveys revealed that the prevalence of neuropathic pain is as high as 8% in the general population, which causes a heavy economic burden to individuals and society [3,4]. Drug treatment remains a common route for pain relief. Unfortunately, available drugs, including antidepressants, anticonvulsants, and opioids, have insufficient efficacy in pain relief and exhibit various side effects [5,6]. Therefore, novel medicines against neuropathic pain should be discovered.

The barely satisfactory effect of conventionally analgesics is

associated with the complex and poorly understood pathogenesis of neuropathic pain. Multiple mechanisms, including oxidative stress and inflammation, involved in neuropathic pain have been found [7,8]. Elevated reactive oxygen species (ROS) levels have been observed in the spinal cord of neuropathic pain animal models [9,10]. Chronic constriction-induced sciatic nerve injury can considerably decrease antioxidant enzyme activities and increase the malondialdehyde (MDA) concentration in the spinal cord under pain conditions [11–13]. Matrix metalloproteinases (MMPs) are responsible for neuropathic pain. In particular, MMP-9 is correlated with oxidative stress and glial cell activation [14–16]. Spinal glial cells, including microglia and astrocytes, are overactivated in neuropathic pain [17]. Nociceptive mediators which play vital roles in neuropathic pain pathogenesis, such as

\* Correspondence to: J. Niu, Ningxia Key Laboratory of Craniocerebral Diseases of Ningxia Hui Autonomous Region, Ningxia Medical University, Yinchuan 750004, PR China

\*\* Correspondence to: J. Yu, Department of Pharmacology, Ningxia Medical University, 1160 Shengli Street, Xingqing, Yinchuan 750004, PR China.

E-mail addresses: [nxmcnjg@163.com](mailto:nxmcnjg@163.com) (J. Niu), [YujqLab@163.com](mailto:YujqLab@163.com) (J. Yu).

<sup>1</sup> Guoxin Zhang and Ning Liu contributed equally to this work.

proinflammatory cytokines, are released by activated microglia and astrocytes [18,19]. ROS produced by peripheral nerve injury activates MMP-9, which in turn activates cytokines such as interleukin-1 $\beta$ , which act on adjacent microglia and astrocytes [20]. Activated glial cells also produce numerous pain-causing substances, such as inflammatory factors, to facilitate central sensitization and maintain neuropathic pain via distinct mechanisms [21,22]. A variety of plant extracts and monomers have been found to exert anti-neuropathic pain through anti-inflammatory and anti-oxidation activities [23]. This information indicates that anti-oxidant and anti-inflammatory agents can inhibit MMP-9 activation, further inhibit glial cell activation, reduce the release of inflammatory factors, and thereby alleviate neuropathic pain. Thus, efficacious and safe natural compounds that treats neuropathic pain by inhibiting oxidative stress, MMP-9 and neuroinflammation should be explored.

Natural herbs have been widely used as sources of medicine. The good therapeutic properties, multitargeted efficacy, low toxicity, and side effects of these plants are recognized well by the masses [24]. Isoorientin (3',4',5,7-tetrahydroxy-6-C-glucopyranosyl flavone) is a common ubiquitous natural product [25], and its chemical structure is shown in Fig. 1. Isoorientin can be separated from several plant species and cereals, such as *Pueraria lobata* (Willd.) Ohwi [26], *Phyllostachys heterocycla* (Carr.) Mitford cv. *pubescens* [27], *Gentiana scabra* Bunge [28], and maize [29]. Isoorientin has shown multiple biological functions, including clearance of ROS [30], inhibition of BV2 microglial inflammatory response [31], and exhibits antitumor [32] and hepatoprotective activities [33]. Isoorientin has shown potentials in docking and binding to MMP-9 and has reduced the MMP-9 expression involved in tumor invasion and metastasis on pancreatic cancer cells [34,35]. Esra et al. [36] reported the anti-inflammatory and analgesic activities of isoorientin against carrageenan-induced hind paw edema and p-benzoquinone-induced abdominal constriction test in mouse models. However, no scientific reports have been published on the analgesic activity of isoorientin in neuropathic pain.

CCI is a commonly used model in preclinical animal studies to simulate the behavioral characteristics and pathological mechanisms of neuropathic pain [37]. Pregabalin is a Food and Drug Administration-approved substance used as the first-line of treatment for neuropathic pain [38]. Pregabalin exhibits nerve protective properties related to myelin sheath degeneration prevention and increase in nerve conduction velocity in neuropathic pain [39]. Therefore, this study was performed to evaluate the antinociceptive efficacy of isoorientin in CCI-induced neuropathic pain in mice and explore the underlying mechanisms of the antinociceptive efficacy of isoorientin. Pregabalin served as a positive control drug.

## 2. Materials and methods

### 2.1. Experimental animals

Adult male specific pathogen-free Institute of Cancer Research (ICR)

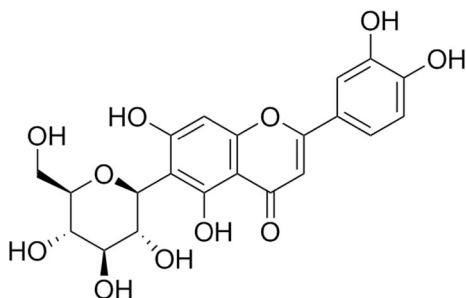


Fig. 1. Chemical structure of isoorientin (ISO). The molecular formula and molecular weight of ISO are  $C_{21}H_{20}O_{11}$  and 448.38, respectively.

mice weighing  $20 \pm 2$  g were provided by the Experimental Animal Center of Ningxia Medical University (Certificate number: SCXK Ningxia 2015-0001). Five mice were kept in a plastic cage with soft bedding and provided food and water ad libitum at  $22^\circ\text{C} \pm 2^\circ\text{C}$  and photoperiods of 12 h/12 h light–dark cycles. The mice were housed properly and acclimated for 3 days before the experiments were performed.

### 2.2. Drugs and chemicals

Isoorientin (purity  $\geq 99.7\%$ ; lot no. P2909F73674; Shanghai Yuanye Corporation) suspended in 0.5% sodium carboxymethyl cellulose was injected intragastrically (i.g.). Sodium pentobarbital was purchased from Sigma-Aldrich (Steinheim, Germany). Pregabalin was obtained from Pfizer Manufacturing Deutschland GmbH (New York, USA). Sodium pentobarbital and pregabalin were dissolved in saline solution. The volume was administered at 10 mL/kg body weight.

### 2.3. CCI model preparation

Surgeries were performed under sterile conditions. The mice received deep anesthesia by the i.p. injection of 0.8% sodium pentobarbital. The CCI operation was performed in accordance with a previous study [40] with slight modifications. In brief, after the skin was shaved and sterilized, the right sciatic nerve was exposed. Three sterile loose ligatures by using 4–0 chromic gut spaced approximately 1 mm were made around the sciatic nerve, and the incision was sutured with 3–0 nonabsorbable silk suture. Sham surgeries were carried out with an identical procedure but without a nerve ligature.

### 2.4. Experimental design

The mice were randomly assigned to the following groups ( $n = 10$ ): sham + vehicle, sham + isoorientin (30 mg/kg/day, i.g.), CCI + vehicle, CCI + pregabalin (40 mg/kg/day, i.g.), and CCI + isoorientin (7.5, 15, and 30 mg/kg/day, i.g.) groups. The doses of isoorientin treatment in this research were determined in accordance with literature reports and our preliminary experiments [27,36]. The protocol of animal study is shown in Fig. 2.

### 2.5. Behavioral examination

Behavioral tests were performed in a randomized and blinded manner and at 9:00 a.m. to 4:00 p.m. after 1 h of administration. In brief, the mice were selected randomly for behavioral experimentation, and observations were conducted by another researcher that was blinded to the status of the mice.

#### 2.5.1. Von Frey filament test

The mechanical withdrawal threshold (MWT) was measured via calibrated nylon von Frey filaments to assess mechanical allodynia [41]. In brief, the mice were acclimatized for 30 min, and the plantar part of the ipsilateral hind paw was stimulated with von Frey fibers by using the up–down method. Stimuli started at 0.4 g and continued until a nociceptive-like response occurred, or the force reached 4.0 g (cut-off value). Paw withdrawal, licking, and shaking were considered as nociceptive-like responses.

#### 2.5.2. Cold plate test

The number of the ipsilateral side hind paw lifted by using the cold plate was assessed [42] to characterize cold allodynia. In brief, the mice were placed in a precooled metal plate at  $4.0^\circ\text{C} \pm 0.5^\circ\text{C}$  and was allowed to acclimatize for 5 min before counting. Cold allodynia was analyzed by recording the total number of hind paw withdrawal, licking, and shaking for 5 min.

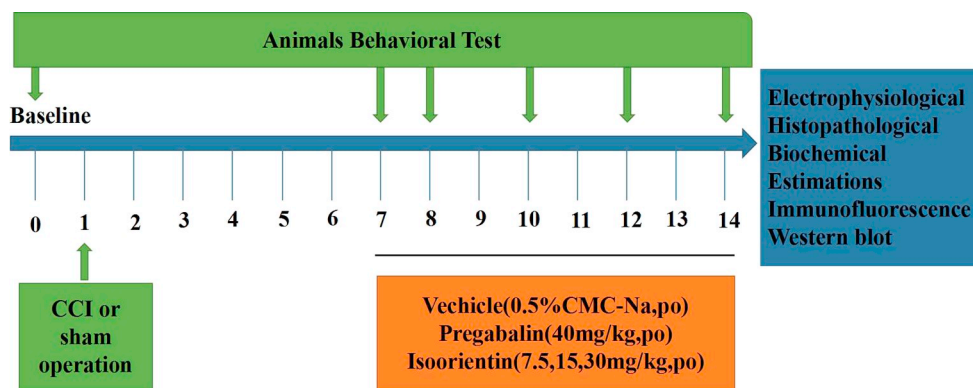


**Fig. 2.** Protocol of animal study. ICR male mice underwent a CCI operation to induce neuropathic pain. Baseline data were recorded 1 day before the CCI operation through behavioral tests. The mice then underwent the CCI operation. After 7 days, they were intragastrically administered with vehicle (10 mL/kg), isoorientin (7.5, 15, or 30 mg/kg), or pregabalin (40 mg/kg) once daily for 8 consecutive days. Behavioral examinations were performed 1 h after drug administration on days 7, 8, 10, 12, and 14 following CCI surgery. After each behavioral examination was conducted, on day 14, electrophysiological analysis, histopathological evaluations, biochemical changes, immunofluorescence analysis, and Western blot assay were performed, and the results were evaluated.

### 2.5.3. Radiant heat test

A radiant heat test was performed to assess thermal hyperalgesia by using a plantar analgesia tester in accordance with a previously described method [43]. In brief, the mice were placed on the glass pane, and the plantar surface was vertically heated by a 5 mm-diameter laser radiant heat source. When the mice withdrew their paw, this movement was detected by using an instrument, and the timer was automatically stopped. Thermal withdrawal latency (TWL) was measured with three consecutive thermal tests performed at least 5 min apart. A cut-off value of 14 s was applied to avoid possible tissue damage.

## 2.6. Electrophysiological examination

### 2.6.1. Sensory nerve conduction velocity (SNCV)

SNCV was measured and recorded in accordance with previous studies [44,45]. In a temperature-controlled environment, the mice were anesthetized by 0.8% sodium pentobarbital i.p. injection. Sural SNCV was measured through the stimulation of the sciatic and sural nerve by using bipolar needle electrodes at a frequency of 0.10 Hz, a duration of 0.2 ms, and a stimulus of 1 V. The distance between stimulating and recording electrodes was determined using a sliding caliper. SNCV (m/s) was calculated as the ratio of the distance between two bipolar recording electrodes (S) to the time difference between two latencies ( $\Delta t$ ,  $V = S/\Delta t$ ). The mice were subjected to electrophysiology tests for < 30 min to avoid possible tissue damage [46,47].

### 2.6.2. Sensory nerve action potential (SNAP) amplitudes

SNAP amplitude was calculated from peak to peak via a previously described method.

## 2.7. Histopathological assessment

### 2.7.1. Hematoxylin and eosin staining

The mice were perfused transcardially with 0.9% saline and with 4% paraformaldehyde after they were anesthetized through the i.p. injection of 80 mg/kg sodium pentobarbital. The sciatic nerves were fixed with 10% formalin at 4 °C overnight. Tissue specimens were then embedded in paraffin, and the paraffin-embedded samples were then mounted in vibratome (Leica, Solms, Germany) and cut into 4  $\mu$ m. The samples from each group (6 mice per group) were stained with hematoxylin and eosin [48]. The sections were observed under  $\times 100$  objective lens using a light microscope (Olympus, Tokyo, Japan) and then images were acquired.

### 2.7.2. Transmission electron microscope

The sciatic nerves were collected using the same method as HE staining and processed for morphological analysis using a transmission

electron microscope. In brief, the sciatic nerves were fixed with 2% glutaraldehyde, dehydrated with graded ethanol solutions, and infiltrated with Epon812. The samples were subsequently embedded with epoxy resin, and the resin-embedded epoxy was then cut at 75 nm. After the samples were stained with 0.4% uranyl acetate and 2% lead citrate, the ultrathin cross-sections were observed under a transmission electron microscope ( $\times 5000$  and  $\times 30,000$ , Hitachi, Tokyo, Japan). Images were randomly obtained in a blinded manner [49,50].

## 2.8. Biochemical estimations

On day 14, the mice were sacrificed after behavioral measurements. The L4–L5 lumbar enlargement spinal cord segments were then immediately removed and homogenized with normal saline by using a glass homogenate and centrifuged at 3000 r/min for 8 min. The supernatant of the homogenate (10%, w/v) was used to detect total antioxidant capacity (T-AOC), total superoxide dismutase (T-SOD), catalase (CAT), and malondialdehyde (MDA) activities in accordance with the instructions from the assay kits (Nanjing Jiancheng Bioengineering Institute, Nanjing, China).

## 2.9. Immunofluorescence analysis

The spinal cord sections were collected using the same method as H & E staining. The sections from each group (6 mice per group) were sequentially transferred to graded alcohols and xylene dehydration and blocked with 10% goat serum for 1 h at room temperature. The sections were then incubated for 2.5 h at 37 °C in phosphate buffered saline (PBS) and primary antibodies in the following dilution ratios: MMP-9 (1:50, Proteintech Group, USA), glial fiber acidic protein (GFAP) (1:100, Proteintech Group, USA), and ionized calcium-binding adaptor molecule-1 (IBA-1) (1:100, Proteintech Group, USA). The sections were then washed with PBS five times, incubated with the fluorescent secondary antibody at 1:100 [FITC-conjugated Affinipure Goat Anti-Rabbit IgG (H + L), Proteintech Group, USA] for 1 h, and washed again with PBS. The cover slips were stained with 40, 6-diamidino-2-phenylindole (DAPI) for 10 min. Images were randomly acquired in a blinded manner using a laser scanning confocal microscope (Olympus FV1000 confocal system) ( $\times 400$ ).

## 2.10. Western blot

On day 14, the mice were decapitated after the behavioral experiments were conducted. L4–L6 spinal cords were rapidly removed and stored at  $-80$  °C until the assay was performed. L4–L6 spinal cord tissues were homogenized using a glass homogenate and a lysis buffer. The lysates were centrifuged at 12,000g and 4 °C for 15 min. The

supernatant was obtained, and the total protein content was measured with a total protein extraction kit. Protein concentrations were analyzed using a BCA protein assay kit (Thermo, USA). The separated proteins (40 µg/lane) were electrophoresed with 12% and 8% SDS/PAGE and transferred to polyvinylidene fluoride membranes. After the membranes blocked with 5% skimmed milk in PBST for 2 h at room temperature and incubated in PBST with primary antibodies (rabbit, IL-1 $\beta$ , 1:2000, Abcam Group, UK; rabbit, tumor necrosis factor- $\alpha$  [TNF- $\alpha$ ], 1:400; rabbit, IL-6, 1:2000) at 4 °C overnight.  $\beta$ -actin (rabbit, 1:2000, Proteintech Group, USA) and tubulin (mouse, 1:1000, Proteintech Group, USA) antibodies were used for the control of the total protein. The membrane was then washed with PBST and incubated with secondary antibodies (goat anti-rabbit IgG, goat anti-mouse IgG, 1:5000; Proteintech Group, USA). Protein signals were visualized using an ECL kit (Applygen technology, Beijing, China). Each protein band was subjected to densitometry analysis via Quantity One software (Bio-Rad Laboratories, Hercules, CA, USA) by an investigator who was blinded to the groups of animals.

### 2.11. Statistical analysis

Data were analyzed with SPSS 24.0 (Chicago, IL). Results were expressed as mean  $\pm$  standard deviation (SD) of at least three independent determinations, where  $n$  indicates the number of experimental animals. In behavioral and electrophysiological studies, the parametrics were statistically analyzed via two-way repeated measure ANOVA and Bonferroni method for post-hoc comparisons. The effects of drug treatment on protein levels were performed through one-way ANOVA with a pairwise comparison via a Tukey–Kramer test. Differences were considered statistically significant at  $P < 0.05$ .

## 3. Results

### 3.1. Effects of isoorientin on CCI-induced neuropathic pain symptoms

First, the CCI-induced neuropathic pain hallmark symptoms were assessed to examine the antinociceptive effects of isoorientin. The results were as follows.

#### 3.1.1. Isoorientin attenuated CCI-induced mechanical allodynia

The influence of isoorientin on MWT is shown in Fig. 3a. The baselines of MWT showed insignificant difference among the groups ( $P > 0.05$ ). The MWT of the CCI group mice significantly decreased compared with that of the sham group on days 7–14 post-surgery ( $P < 0.01$ ). The drugs were administered for 8 consecutive days from day 7 post-CCI surgery in each group. The MWT was attenuated after isoorientin administration in a dose-dependent manner. Pregabalin

treatment (40 mg/kg) also produced similar effects ( $P < 0.01$ ). Additionally, sham + isoorientin (30 mg/kg) group did not significantly differ from the sham group in terms of MWT ( $P > 0.05$ ).

#### 3.1.2. Isoorientin attenuated CCI-induced cold allodynia

The influence of isoorientin on paw lifts is shown in Fig. 3b. The baselines of the counts of paw withdrawal were not significantly different among the groups ( $P > 0.05$ ). In comparison with the sham group, the CCI-induced cold allodynia was significantly increased on 7th day post-surgery and sustained throughout the duration of the study ( $P < 0.01$ ). The number of paw withdrawal markedly decreased in a dose-dependent manner in the isoorientin-treated group compared with those in the CCI group. Pregabalin (40 mg/kg) treatment also produced similar effects ( $P < 0.01$ ). Additionally, the counts of paw withdrawal were observed in the sham + isoorientin (30 mg/kg) group and did not have significant differences compared with those in the sham group ( $P > 0.05$ ).

#### 3.1.3. Isoorientin attenuated CCI-induced thermal hyperalgesia

The influence of isoorientin on TWL is shown in Fig. 3c. Our data indicated that the baseline values of the TWL insignificant group differences before surgery ( $P > 0.05$ ). As expected, the CCI mice exhibited thermal hyperalgesia 7 days after the surgery ( $P < 0.01$ ). They were intragastrically administered with isoorientin significantly decreased CCI-induced TWL in a dose-dependent manner ( $P < 0.01$ ), and pregabalin (40 mg/kg) treatment produced similar effects ( $P < 0.01$ ). In the sham + isoorientin (30 mg/kg) group, the withdrawal latency of the mice from the thermal stimulus did not change compared with that in the sham group ( $P > 0.05$ ).

### 3.2. Effects of isoorientin on SNCV and SNAP amplitudes

The results of the electrophysiological experiments on SNCV and SNAP amplitudes are shown in Fig. 4. In comparison with the sham group, CCI significantly decreased the SNCV and SNAP amplitudes ( $P < 0.01$ ). Nevertheless, the sham + isoorientin (30 mg/kg) group did not significantly differ from the sham group in terms of SNCV and SNAP amplitudes ( $P > 0.05$ ). The repeated administration of pregabalin (40 mg/kg) and isoorientin (7.5, 15, and 30 mg/kg) led to an improvement in CCI-induced SNCV and SNAP amplitudes compared with that of the CCI group on day 14 (Figs. 4a–g). These observations revealed that isoorientin could restore the CCI-induced nerve conduction function disorder but did not influence the nerve conduction function of the sham mice.

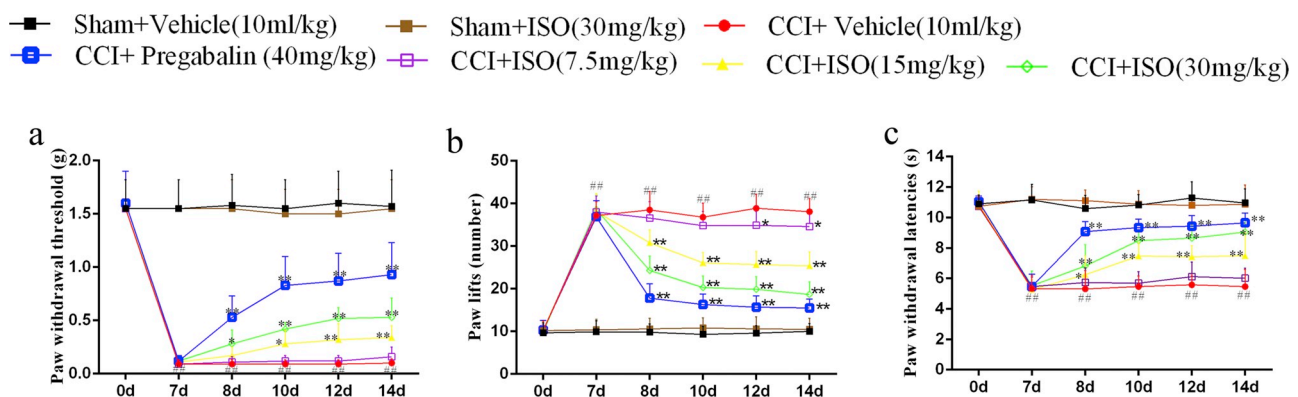
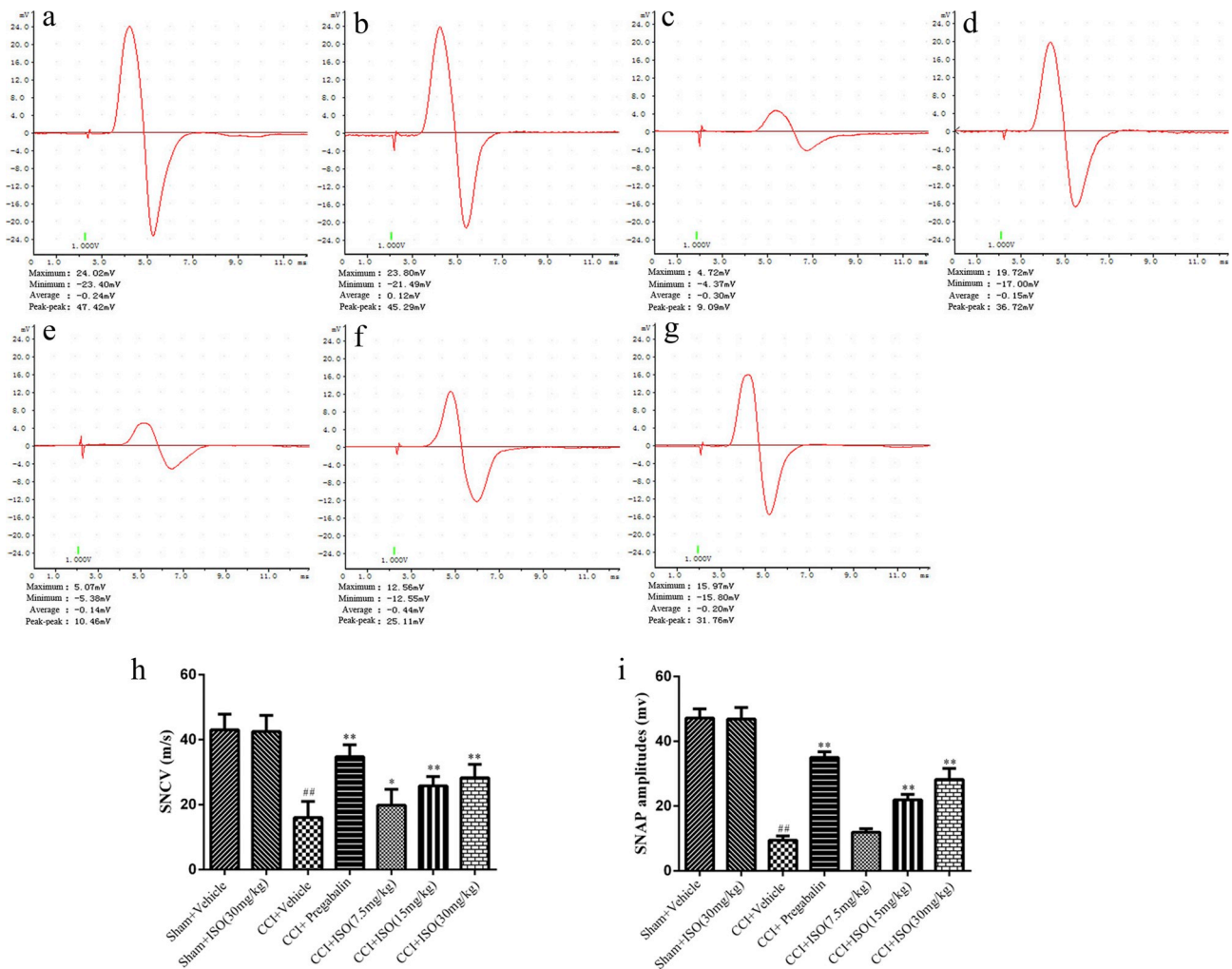


Fig. 3. Effects of isoorientin on behavioral alterations in CCI-induced neuropathic pain. (a) Effect of isoorientin on mechanical allodynia in von Frey filaments test. (b) Effect of isoorientin on cold allodynia in a cold plate test. (c) Effect of isoorientin on thermal hyperalgesia in a radiant heat test. Data were expressed as mean  $\pm$  SD ( $n = 6$ ); ##  $P < 0.01$  versus sham group; \* $P < 0.05$ , \*\* $P < 0.01$  versus the CCI group.



**Fig. 4.** Effects of isoorientin on electrophysiological alterations of the sciatic nerve in CCI-induced neuropathic pain. Representative traces of SNAP of the sciatic sural nerve on day 14 are shown in (a–g). (a) SNAP trace of the sham group. (b) SNAP trace of the sham + isoorientin 30 mg/kg group. (c) SNAP trace of the CCI group. (d) SNAP trace of the pregabalin (40 mg/kg) group. (e) SNAP trace of the 7.5 mg/kg isoorientin group. (f) SNAP trace of the 15 mg/kg isoorientin group. (g) SNAP trace of the 30 mg/kg isoorientin group. (h) Effects of isoorientin on SNCV. (i) Effects of isoorientin on SNAP amplitudes. Data were expressed as mean ± SD (n = 6). ##P < 0.01 versus the sham group, \*P < 0.05, \*\*P < 0.01 versus the CCI group.

### 3.3. Effect of isoorientin on CCI-induced histopathological changes

#### 3.3.1. H&E staining

The cross-section of the sciatic nerve was stained with H&E to examine whether isoorientin attenuated the histological change in the

sciatic nerve (Fig. 5 and Table 1). In comparison with the sham group, the myelinated nerve fibers were disordered, the axons were swollen, and the neuron gaps were created in the CCI group (Figs. 5a and c). However, dose-dependent isoorientin (15 and 30 mg/kg) treatment ameliorated the CCI-induced histopathological changes (Figs. 5f–g).

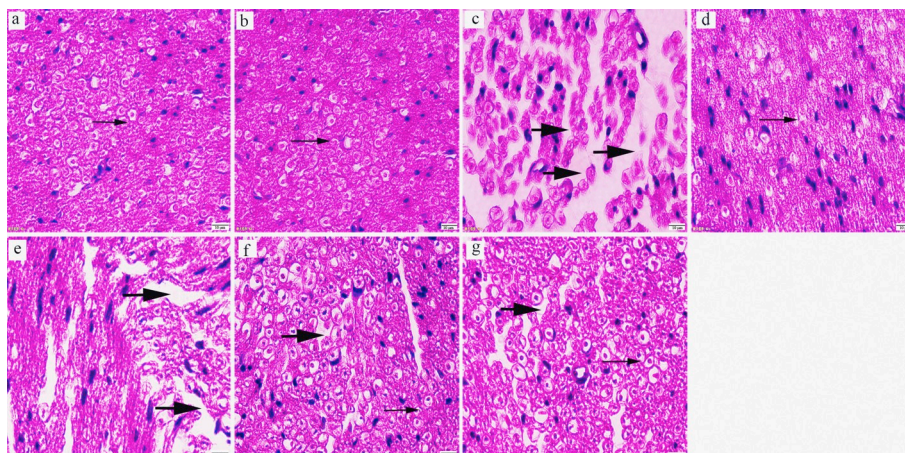


**Fig. 5.** Effects of isoorientin on the histopathological alterations of the sciatic nerve in CCI-induced neuropathic pain as shown by H&E staining. (a)–(g) show the sciatic nerve cross-sections from the sham, sham + isoorientin (30 mg/kg), CCI, CCI + pregabalin (40 mg/kg), and CCI + isoorientin (7.5, 15, and 30 mg/kg) treatment groups, respectively. In the images, the thin and thick black arrows show fiber arrangement and neuron gaps, respectively. Microscopic analysis was performed under a light microscope at a magnification of ×1000 and a scale bar of 10 μm.

**Table 1**  
Effect of isoorientin on tissue architecture of sciatic nerve in CCI-induced neuropathic pain.

Groups	Nerve fiber derangement	Axonal abnormal swelling	Neuron gaps extent
Sham	–	–	–
Sham + isoorientin (30 mg/kg)	–	–	–
CCI	++	++	++
CCI + pregabalin (40 mg/kg)	–	–	+
CCI + isoorientin (7.5 mg/kg)	++	++	++
CCI + isoorientin (15 mg/kg)	+	+	+
CCI + isoorientin (30 mg/kg)	–	+	+

(–) Nil, (++) Severe, (+) Mild.

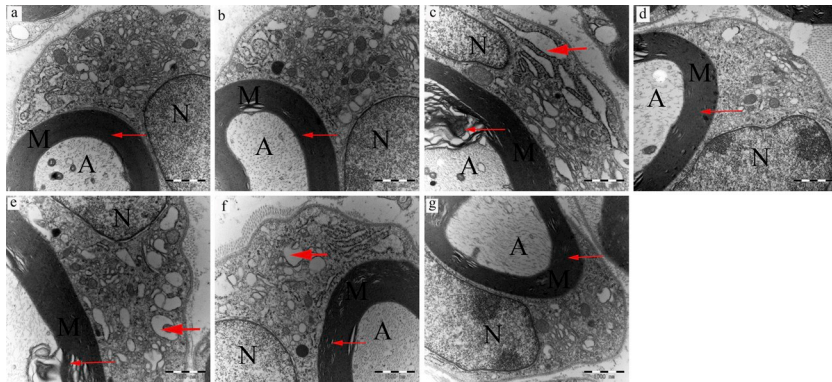


**Fig. 6.** Ultrastructure of the sciatic nerve in mice examined under TEM ( $\times 30,000$  magnification; bar =  $1 \mu\text{m}$ ). (a)–(g) represent the sciatic nerve cross-sections from sham, sham + isoorientin (30 mg/kg), CCI, CCI + pregabalin (40 mg/kg), and CCI + isoorientin (7.5, 15, and 30 mg/kg) treated groups, respectively. A-axon, M-myelin lamina, and N-Schwann cell nucleus. In the images, the thin and thick red arrows show myelin sheath and organelle vacuoles, respectively. (For interpretation of the references to color in this figure legend, the reader is referred to the web version of this article.)

The pregabalin (40 mg/kg) treatment elicited similar effects (Fig. 5d). The sham + isoorientin (30 mg/kg) group did not significantly differ from the sham group (Figs. 5a–b).

### 3.3.2. Transmission electron microscopy

Variations in the sciatic nerve ultrastructure were observed through transmission electron microscopy to determine whether the alteration of electrophysiological reaction was due to the neuroprotective effect of isoorientin. Fig. 6 shows the sciatic nerve ultrastructure under  $30,000 \times$  magnification. Figs. 7a–g illustrate this ultrastructure under  $5000 \times$  magnification. Fig. 7h shows the percentage of the abnormal

myelin sheath (%). The myelin sheaths had an intact structure and were densely arranged in the sham group. However, the abnormal ultrastructure of the sciatic nerve indicated that the myelin sheath exhibited segmental demyelination and lamellar separation, axonal swelling, and numerous vacuoles of organelles occurred in the CCI group. By contrast, isoorientin treatment could ameliorate the abnormal ultrastructure of the sciatic nerve and reduce the abnormal myelin sheath percentage (%) ( $P < 0.01$  for the mice treated with 30 mg/kg isoorientin and  $P < 0.05$  for the mice administered with 15 mg/kg isoorientin; Fig. 7h). The treatment with 40 mg/kg pregabalin also showed a similar effect. The sham + isoorientin (30 mg/kg) group did not significantly

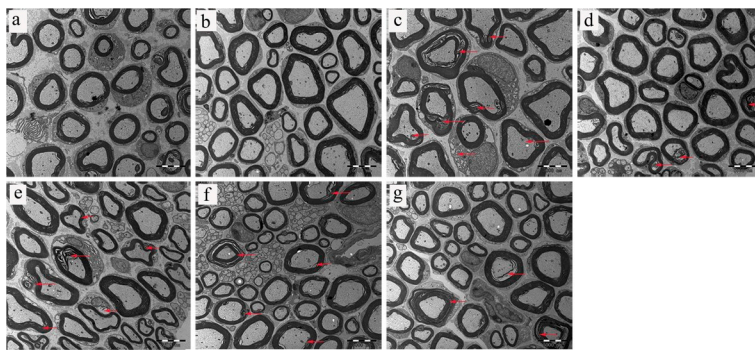


**Fig. 7.** Ultrastructure of the sciatic nerve in mice were examined under transmission electron microscopy ( $\times 5000$  magnification; bar =  $5 \mu\text{m}$ ); each group consists of six mice ( $n = 6$ ). (a–g) Data of the cross-sections of the sciatic nerve from sham, sham + isoorientin (30 mg/kg), CCI, CCI + pregabalin (40 mg/kg), and CCI + isoorientin (7.5, 15, and 30 mg/kg) treated groups, respectively. (h) Data of the abnormal myelin sheath and axons (%). In the images, the thin red arrows show abnormal myelin sheath and axons. Results expressed as mean  $\pm$  SD ( $n = 6$ ); ## $P < 0.01$  versus the sham group; \* $P < 0.05$ , \*\* $P < 0.01$  versus the CCI group. (For interpretation of the references to color in this figure legend, the reader is referred to the web version of this article.)

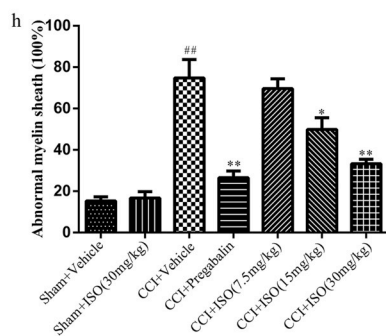


**Table 2**  
The levels of T-AOC, CAT, T-SOD and MDA in the spinal cord of neuropathic pain mice.

Groups	Dose (mg/kg)	T-AOC U/mgprot	CAT U/mgprot	T-SOD U/mgprot	MDA U/mgprot
Sham	–	1.41 ± 0.12	20.38 ± 3.06	226.27 ± 21.19	3.03 ± 0.55
CCI	–	0.68 ± 0.19 <sup>##</sup>	16.16 ± 1.90 <sup>##</sup>	145.51 ± 35.95 <sup>##</sup>	4.42 ± 0.56 <sup>##</sup>
CCI + Isoorientin	30	1.20 ± 0.18 <sup>**</sup>	18.19 ± 1.92 <sup>*</sup>	201.95 ± 13.46 <sup>**</sup>	3.37 ± 0.28 <sup>**</sup>
	15	0.98 ± 0.23 <sup>*</sup>	18.00 ± 2.71 <sup>*</sup>	195.63 ± 27.04 <sup>**</sup>	3.33 ± 0.36 <sup>**</sup>
	7.5	0.89 ± 0.25	17.54 ± 2.35	174.27 ± 28.89	4.09 ± 0.95

Data are expressed as mean ± SD (n = 6).

<sup>##</sup> *P* < 0.01 compared with the sham group.

<sup>\*</sup> *P* < 0.05.

<sup>\*\*</sup> *P* < 0.01 compared with the CCI group.

differ from the sham group (Figs. 6a–b and 7a–b).

### 3.4. Effect of isorientin on oxidative stress markers

The influences of isorientin on T-AOC, CAT, T-SOD, and MDA in the spinal cord are shown in Table 2. In the CCI group, the levels of T-AOC (*P* < 0.01), CAT (*P* < 0.01), and T-SOD (*P* < 0.01) decreased, and the MDA concentrations markedly increased (*P* < 0.01) compared with that in the sham group. Isoorientin (30 and 15 mg/kg) administration significantly increased T-AOC (*P* < 0.01; *P* < 0.05), CAT (*P* < 0.05), and T-SOD levels (*P* < 0.01) and decreased the MDA concentrations (*P* < 0.01). However, isorientin (7.5 mg/kg) administration did not significantly differ (*P* > 0.05). The data suggested that chronic treatment with isorientin could inhibit CCI-induced oxidative stress in the spinal cord.

### 3.5. Effects of isorientin on the MMP-9 expression

The most effective dose of isorientin was determined to be 30 mg/kg after assessing all the results of the experiments above; thus, the mice receiving this dose were chosen for immunofluorescence and Western blot analysis. The spinal cord sections were stained with an antibody for MMP-9 to explore the effects of isorientin on the MMP-9

expression. The green signal indexed the MMP9-positive cells stained with FITC, and the cell nucleus stained with DAPI were indexed red. Fig. 8 shows that the ratio of the MMP9-positive cells to the nucleus in the CCI group was significantly higher than that in the sham group (*P* < 0.01). However, the MMP-9 expression in the CCI + isorientin (30 mg/kg) group was dramatically lower than that in the CCI mice (*P* < 0.01). The data revealed that the repeated administration of 30 mg/kg isorientin could inhibit the MMP-9 expression in the spinal cord of the CCI mice.

### 3.6. Effects of isorientin on glial cell expression

IBA-1 and GFAP are markers for microglia and astrocytes, whose upregulation indicated microglial and astrocyte activation. IBA-1 and GFAP expression levels in the spinal cord were examined through immunofluorescence with anti-IBA-1 and anti-GFAP antibodies to determine the effects of isorientin on glial cell activation (Fig. 9). The green and red signals represent FITC-tagged IBA-1 and GFAP and the DAPI-tagged nucleus, respectively. Immunofluorescence analysis showed that the expression levels of IBA-1 and GFAP in the CCI group were markedly higher than those in the sham group (*P* < 0.01). By contrast, the expression levels of IBA-1 and GFAP in the CCI + isorientin (30 mg/kg) group were significantly lower than those in the

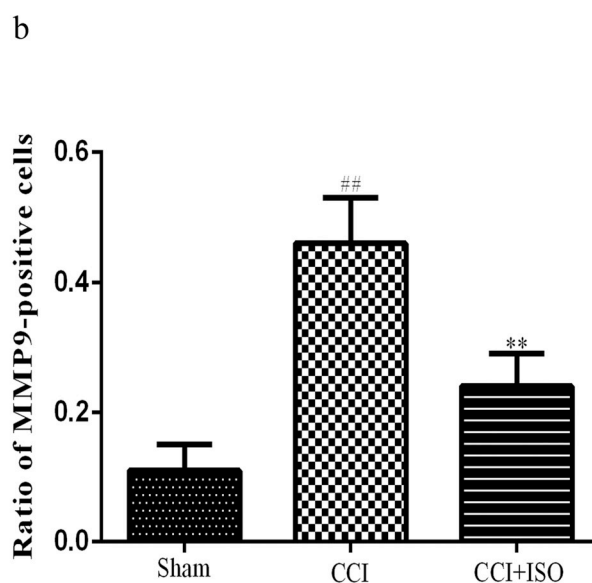
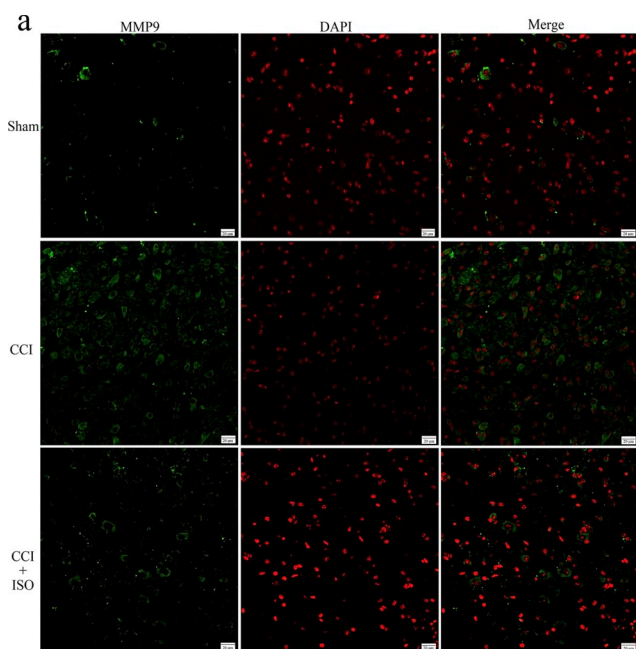


**Fig. 8.** Isoorientin (30 mg/kg) inhibited the MMP-9 expression in CCI mice. (a) Photomicrographs of MMP-9 immunofluorescence staining in the spinal cord (×400). (b) Quantitative analysis of the ratio of MMP-9-positive cells to the nucleus. Data expressed as mean ± SD (n = 6). <sup>##</sup>*P* < 0.01 versus the sham group, <sup>\*\*</sup>*P* < 0.01 versus the CCI group.

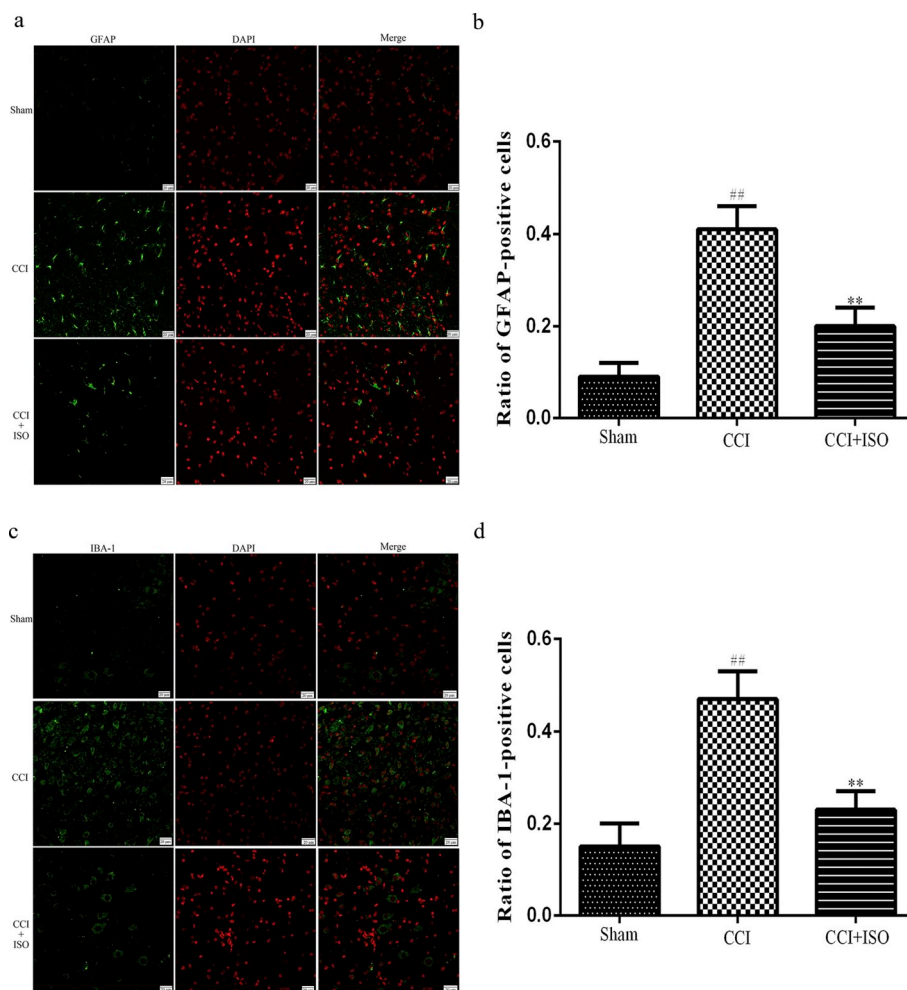


**Fig. 9.** Isoorientin (30 mg/kg) inhibited the activation of astrocytes and microglia in CCI mice. (a) and (c) Photomicrographs of astrocytes and microglial immunofluorescence staining in the spinal cord ( $\times 400$ ), respectively. (b) and (d) Quantitative analysis of the ratio of GFAP-positive and IBA-1-positive cells to the nucleus, respectively. Data expressed as mean  $\pm$  SD ( $n = 6$ ). <sup>##</sup> $P < 0.01$  versus the sham group, <sup>\*\*</sup> $P < 0.01$  versus the CCI group.

CCI group ( $P < 0.01$ ). In summary, our results indicated that the chronic treatment with 30 mg/kg isoorientin could suppress CCI-induced astrocyte and microglial overactivation.

### 3.7. Effects of isoorientin on pro-inflammatory factor expressions

The expression levels of TNF- $\alpha$ , IL-6, and IL-1 $\beta$  in the L4–L5 specimens spinal cord were measured via Western blot analysis to determine the isoorientin expression on CCI-induced pro-inflammatory cytokine (Figs. 10a–c). Our data revealed that TNF- $\alpha$ , IL-6, and IL-1 $\beta$  levels in the CCI group were markedly higher than those in the sham group ( $P < 0.01$ ). The chronic administration of 30 mg/kg isoorientin significantly downregulated the protein expressions of TNF- $\alpha$ , IL-6, and IL-1 $\beta$  in the CCI mice spinal cord ( $P < 0.01$ ). These data indicated that the 30 mg/kg chronic treatment of isoorientin could inhibit CCI-induced neuroinflammation.

## 4. Discussion

Neuropathic pain is a chronic pain syndrome caused by disease or damage of the nervous system, usually accompanied by abnormal sensation, abnormal electrophysiological response and neurologic impairment [51–53]. Millions of people suffer from neuropathic pain, but its treatment and diagnosis remain insufficient. Oxidative stress and inflammation have been proposed in causative and deteriorative roles in neuropathic pain [54]. Isoorientin is a well-known flavonoid-like

compound that exerts multiple pharmacological activities, such as antioxidant and anti-inflammatory functions [33,55,56]. The antinociceptive, anti-inflammatory, and antiulcerogenic activities of isoorientin have been confirmed in rat and mouse models [36]. In the current study, the antinociceptive activities of isoorientin were shown in the mice with CCI, and no remarkable toxicity reaction was observed in normal mice.

The CCI model has been confirmed and frequently used to assess neuropathic pain in vivo by mimicking the pathological effect of neuropathic pain in humans [57,58]. CCI-induced damage exacerbates pain symptoms (i.e., allodynia and hyperalgesia), electrophysiological responses (i.e., sensory nerve action potential amplitude and conduction velocity), and biochemical changes (i.e., reduction in CAT and increase in MDA) [49,59,60]. MMP-9 and glial cells are overactivated, and inflammatory cytokines are overexpressed in the spinal cord; this observation has been demonstrated in CCI-induced neuropathic pain [61,62]. Our successfully established the CCI mouse model, and the CCI-induced histopathological, electrophysiological, and biochemical alternations are consistent with our earlier findings and reports from previous studies [11,49,50].

The mice with CCI showed allodynia and hyperalgesia, which are typical characteristics of neuropathic pain [63–65]. Peripheral and central sensitizations are important mechanisms that lead to allodynia and hyperalgesia behavioral changes under pain conditions [66]. After injuries or dysfunctions in the somatosensory system, cytokines, substance P, and other algogenic substances invade an injured tissue area,

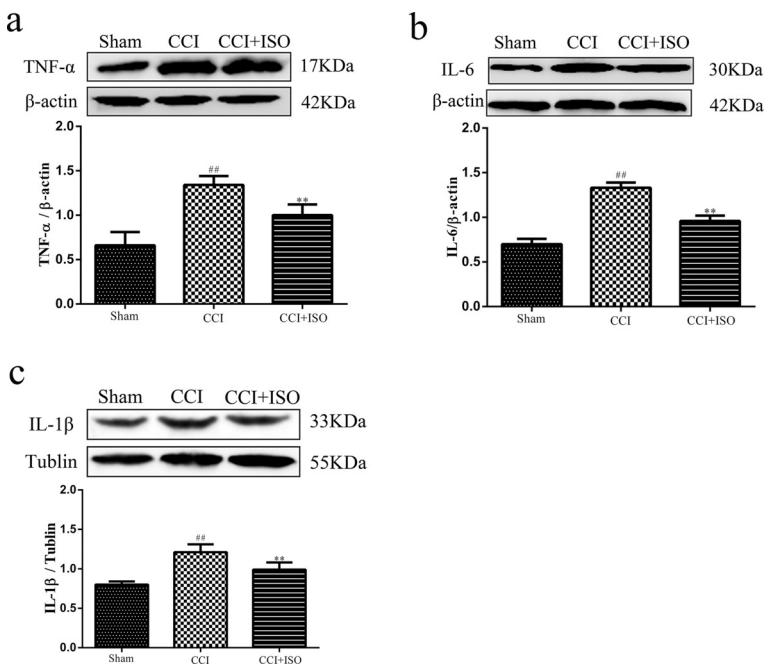


**Fig. 10.** (a–c) Effects of isoorientin on the expression of inflammatory cytokines (TNF- $\alpha$ , IL-6, and IL-1 $\beta$ ) in the spinal cord tissues of CCI-induced neuropathic mice. Western blot analysis of sham + vehicle, CCI + vehicle, and CCI + isoorientin (30 mg/kg) groups. Data expressed as mean  $\pm$  SD (n = 6). <sup>##</sup>*P* < 0.01 versus the sham group, <sup>\*\*</sup>*P* < 0.01 versus the CCI group.

which contributes to peripheral and central sensitization by increasing the sensitivity and excitability of primary sensory neurons and synaptic plasticity in the central nervous system [67,68]. Central sensitization is also driven by glial cell neuroinflammation, which plays a sufficient role in hyperalgesia and allodynia [69,70]. In the present study, isoorientin (15 and 30 mg/kg/day, i.g.) efficiently attenuated the thermal hyperalgesia and mechanical and cold allodynia compared with that of the CCI group. Our findings might suggest that the chronic consecutive isoorientin treatment elicits antinociceptive effect on mice with neuropathic pain induced by CCI.

Peripheral nerve constriction commonly causes the loss of sensory function, which is mainly connected to nerve fiber structure damage. Electrophysiological testing is a common method to study the functional recovery after nerve injury [71]. SNCV and SNAP are often used to determine the status of sensory nerves in all the parameters measured in nerve conduction studies. SNCV accurately reflects myelin integrity and axon caliber, whereas SNAP amplitude indicates the degree of axonotmesis [72]. The demyelination of the sensory fibers results in slowing SNCV and decreasing SNAP amplitude. Axonal degeneration also decreases SNAP amplitude by the loss of conductive elements, although surviving axons function normally [47]. By contrast, in the present study, isoorientin effectively increased SNCV and SNAP amplitude after CCI surgery. In summary, the findings might show that the continuous intragastric administration of isoorientin could ameliorate nerve damage against CCI.

Histopathological evaluations were performed to support the neuroprotective property of isoorientin by observing the changes in nerve fibers, axons, and neurons. In our study, the H&E staining of sciatic nerve sections clearly showed the disordered arrangement of myelinated nerve fibers and numerous neuronal gaps after CCI operation. TEM on the sciatic nerve ultrastructure also showed myelin disintegration, axon separation, and swelling in Schwann organelles. However, the CCI-induced histomorphological changes were markedly improved after isoorientin was administered. Therefore, the damaged axon and myelin were restored by isoorientin, which provided significant evidence that isoorientin had neuroprotective effects.

Oxidation products were increased and caused damage to the nervous tissue in the continuous peroxidative stress reaction of the nervous system, which is an important cause of hyperalgesia and allodynia in neuropathic pain [12]. Superoxide dismutase and CAT, which are

crucial to maintain the balance between oxidative and peroxidative systems, are important antioxidant enzymes that scavenge free radicals and prevent and relieve peroxidative stress reaction. Therefore, the activity of these two enzymes can indirectly reflect the ability to scavenge free radicals. T-AOC is the embodiment of the overall antioxidant level, and its level reflects the function of the antioxidant system. MDA is a lipid peroxidation product generated when free radicals attack tissue cells *in vivo* and cause oxidative damage [73,74]. In the present study, T-AOC, T-SOD, and CAT levels decreased, and MDA levels increased after CCI in the mice. However, the levels of oxidative stress markers were restored in the mice with CCI by isoorientin treatment. The results showed that isoorientin alleviated CCI-induced neuropathic pain that could be involved its antioxidant activity.

MMP-9 is a key molecular protein that maintains neuropathic pain development, which is associated with oxidative stress and neuroinflammation [75,76]. ROS produced at the injury site can activate MMP-9. ROS inhibitor and *N*-acetyl-cysteine suppress the MMP-9 expression to attenuate neuropathic pain [31,77,78]. Activated MMP-9 is sufficient and required in glial cell activation via proinflammatory cytokines, such as IL-1 $\beta$  signaling [15,61,79]. In our investigation, the immunofluorescence analysis showed that the MMP-9 expression was remarkably reduced after the isoorientin administration significantly increased after CCI operation. Isoorientin treatment significantly reduced the CCI-induced overactivation of astrocytes and microglia.

After glial cells are activated, signaling molecules, such as proinflammatory factors, including TNF- $\alpha$ , IL-1 $\beta$ , and IL-6, are released [21]. These cytokines can also activate the nearby glia or neurons to facilitate neuroinflammation via a positive feedback mechanism and enhance peripheral and/or central sensitization and nerve injury-induced persistent pain [68,80]. The expression levels of proinflammatory cytokines IL-6, IL-1 $\beta$ , and TNF- $\alpha$  increase in the spinal cord in neuropathic pain animal models, and the corresponding use of antagonist significantly reduces the proinflammatory cytokine levels and attenuate neuropathic pain [81]. In our study, isoorientin treatment significantly decreased the high CCI-induced IL-6, IL-1 $\beta$ , and TNF- $\alpha$  expression. These findings indicated that isoorientin could notably suppress CCI-induced neuroinflammation.

Pregabalin is developed as a gabapentin derivative and has shown clinical and laboratory efficacies for neuropathic pain [82–84]. Similar to gabapentin, pregabalin functions as an analgesic by binding to the

$\alpha_2\text{-}\delta$  subunit of calcium channels, and inhibit neurotransmitter release [85,86]. Furthermore, pregabalin exhibits nerve-protecting properties that are related to myelin sheath degeneration prevention and increase in nerve conduction velocity in neuropathic pain [87,88]. Thus, pregabalin is the positive control drug in our study.

In summary, our results demonstrated that isorientin exerted antinociceptive and neuroprotective effects on CCI-induced neuropathic pain in mice with CCI via behavioral, electrophysiological, histopathological, biochemical, and molecular experiments. Isoorientin is a potential candidate drug for neuropathic pain treatment. However, several other mechanisms might be involved in isorientin-mediated antineuropathic effects. Therefore, preclinical and clinical studies should be further conducted to confirm the antineuropathic effects of isorientin and elucidate the complete mechanisms of its effectiveness under various painful conditions.

## Declaration of Competing Interest

All authors declared no potential conflicts of interest.

## Acknowledgment

This work was supported by the National Natural Science Foundation of China [Grant numbers: 81360182 and 81660261], the Natural Science Foundation of Ningxia [Grant number: 2019AAC03097], the Major Research and Construction Programs of Ningxia Province [Grant Number: 2017BY079], and the Domestic First-class Project of Traditional Chinese Medicine of Ningxia Medical University of Ningxia Education Department [Grant Number: NXYLXK2017A06].

## Ethics statement

All experimental procedures were strictly performed in accordance with the regulations of the Ethics Committee of the International Association for the Study of Pain (Zimmermann, 1983) and National Guidelines for the Care and Use of Laboratory Animals (The Ministry of Science and Technology of China, 2006). This research was approved by the Animal Ethical Committee of Ningxia Medical University.

## References

- [1] M. Haanpää, N. Attal, M. Backonja, R. Baron, M. Bennett, D. Bouhassira, G. Cruccu, P. Hansson, J.A. Haythornthwaite, G.D. Iannetti, T.S. Jensen, T. Kauppila, T.J. Nurmiikko, A.S.C. Rice, M. Rowbotham, J. Serra, C. Sommer, B.H. Smith, R.-D. Treede, NeuPSIG guidelines on neuropathic pain assessment, *Pain* 152 (2011) 14–27, <https://doi.org/10.1016/j.pain.2010.07.031>.
- [2] I. Gilron, R. Baron, T. Jensen, Neuropathic pain: principles of diagnosis and treatment, *Mayo Clin. Proc.* 90 (2015) 532–545, <https://doi.org/10.1016/j.mayocp.2015.01.018>.
- [3] A. Sra, P.A. Smith, Etiology and pharmacology of neuropathic pain, *Pharmacol. Rev.* 70 (2) (2018) 315–347, <https://doi.org/10.1124/pr.117.014399>.
- [4] O. Van Hecke, S. Austin, R. Khan, B. Smith, Torrance, Neuropathic pain in the general population: a systematic review of epidemiological studies, *Pain* 155 (9) (2014) 654–662, <https://doi.org/10.1016/j.pain.2014.06.006>.
- [5] E. Kalso, D.J. Aldington, R.A. Moore, Drugs for neuropathic pain, *BMJ* 347 (2013) f7339, <https://doi.org/10.1136/bmj.f7339>.
- [6] R. Baron, A. Binder, G. Wasner, Neuropathic pain: diagnosis, pathophysiological mechanisms, and treatment, *Lancet Neurol.* 9 (2010) 807–819, [https://doi.org/10.1016/S1474-4422\(10\)70143-5](https://doi.org/10.1016/S1474-4422(10)70143-5).
- [7] Abolfazl. Abbaszadeh, Saeideh. Darabi, Amin. Hasanvand, Hossein. Amini-Khooei, Amir. Abbaszadeh, Razieh. Choghakhorri, Asghar Aaliehpour, Minocycline through attenuation of oxidative stress and inflammatory response reduces the neuropathic pain in a rat model of chronic constriction injury, *Iran J Basic Med Sci* 21 (2018) 138–144, <https://doi.org/10.22038/IJBMS.2017.24248.6053>.
- [8] H.A. Safakhah, K.N. Moradi, A. Bazargani, A.R. Bandegi, P.H. Gholami, B. Khoshkholgh-Sima, A. Ghanbari, Forced exercise attenuates neuropathic pain in chronic constriction injury of male rat: an investigation of oxidative stress and inflammation, *J. Pain Res.* 10 (2017) 1457–1466, <https://doi.org/10.2147/JPR.S135081>.
- [9] H.K. Kim, S.K. Park, J.L. Zhou, G. Tagliatalata, J.M. Chung, Reactive oxygen species (ROS) are involved in enhancement of NMDA-receptor phosphorylation in animal models of pain, *Pain* 111 (1–2) (2004) 116–124, <https://doi.org/10.1016/j.pain.2004.06.008>.

- [10] Alice Bittar, Jaebom Jun, Jun-Ho La, Jigong Wang, Joong Woo Leem, Jin Mo Chung, Reactive oxygen species affect spinal cell type-specific synaptic plasticity in a model of neuropathic pain, *Pain* 158 (2017) 2137–2146, <https://doi.org/10.1097/j.pain.0000000000001014>.
- [11] Y.-Q. Xu, S.-J. Jin, N. Liu, Y.-X. Li, J. Zheng, L. Ma, J. Du, R. Zhou, C.-J. Zhao, Y. Niu, T. Sun, J.-Q. Yu, Aloperine attenuated neuropathic pain induced by chronic constriction injury via anti-oxidation activity and suppression of the nuclear factor kappa B pathway, *Biochem. Biophys. Res. Commun.* 451 (2014) 568–573, <https://doi.org/10.1016/j.bbrc.2014.08.025>.
- [12] Nitya N. Pathak, Venkanna Balaganur, Madhu C. Lingaraju, Vinay Kant, Najeeb Latief, Amar S. More, Dharendra Kumar, Dinesh Kumar, Surendra K. Tandan, Atorvastatin attenuates neuropathic pain in rat neuropathy model by down-regulating oxidative damage at peripheral, spinal and supraspinal levels, *Neurochem. Int.* 68 (2014) 1–9, <https://doi.org/10.1016/j.neuint.2014.01.014>.
- [13] B.-S. Zhao, L.-X. Meng, Y.-Y. Ding, Y.-Y. Cao, Hyperbaric oxygen treatment produces an antinociceptive response phase and inhibits astrocyte activation and inflammatory response in a rat model of neuropathic pain, *J. Mol. Neurosci.* 53 (2014) 251–261, <https://doi.org/10.1007/s12031-013-0213-3>.
- [14] S.E. Lakhani, M. Avramut, Matrix metalloproteinases in neuropathic pain and migraine: friends, enemies, and therapeutic targets, *Pain Res. Treat.* 2012 (2012) 1–10, <https://doi.org/10.1155/2012/952906>.
- [15] A. Kuhad, P. Singh, K. Chopra, Matrix metalloproteinases: potential therapeutic target for diabetic neuropathic pain, *Expert Opin. Ther. Targets* 19 (2) (2015) 177–185, <https://doi.org/10.1517/14728222.2014.960844>.
- [16] E. Rojewska, W. Makuch, B. Przewlocka, J. Mika, Minocycline prevents dynorphin-induced neurotoxicity during neuropathic pain in rats, *Neuropharmacology* 86 (2014) 301–310, <https://doi.org/10.1016/j.neuropharm.2014.08.001>.
- [17] F.Y. Tanga, V. Raghavendra, J.A. DeLeo, Quantitative real-time RT-PCR assessment of spinal microglial and astrocytic activation markers in a rat model of neuropathic pain, *Neurochem. Int.* 45 (2004) 397–407, <https://doi.org/10.1016/j.neuint.2003.06.002>.
- [18] H. Cao, Y.Q. Zhang, Spinal glial activation contributes to pathological pain states, *Neurosci. Biobehav. Rev.* 32 (5) (2008) 972–983, <https://doi.org/10.1016/j.neubiorev.2008.03.009>.
- [19] J.Y. Lee, H.Y. Choi, B.-G. Ju, T.Y. Yune, Estrogen alleviates neuropathic pain induced after spinal cord injury by inhibiting microglia and astrocyte activation, *Biochim. Acta Mol. Basis Dis.* 1864 (2018) 2472–2480, <https://doi.org/10.1016/j.bbdis.2018.04.006>.
- [20] A.M. Jurga, P. Anna, M. Wioletta, P. Barbara, M. Joanna, Blockade of P2X4 receptors inhibits neuropathic pain-related behavior by preventing MMP-9 activation and, consequently, pronociceptive interleukin release in a rat model, *Front. Pharmacol.* 8 (2017), <https://doi.org/10.3389/fphar.2017.00048>.
- [21] J. Mika, M. Zychowska, K. Popiolek-Barczyk, E. Rojewska, B. Przewlocka, Importance of glial activation in neuropathic pain, *Eur. J. Pharmacol.* 716 (2013) 106–119, <https://doi.org/10.1016/j.ejphar.2013.01.072>.
- [22] J.S. Gwak, J. Kang, G.C. Unabia, C.E. Hulsebosch, Spinal and temporal activation of spinal glial cells: role of gliopathy in central neuropathic pain following spinal cord injury in rats, *Exp. Neurol.* 234 (2012) 362–372, <https://doi.org/10.1016/j.expneurol.2011.10.010>.
- [23] S.S. Quintans Jullyana, R. Antonioli Angelo, R.G.S. Almeida Jackson, J. Santana-Filho Valter, J. Quintans-Júnior Lucindo, Natural products evaluated in neuropathic pain models - a systematic review, *Basic Clin. Pharmacol. Toxicol.* 114 (2014) 442–450, <https://doi.org/10.1111/bcpt.12178>.
- [24] F. Forouzanfar, H. Hosseinzadeh, Medicinal herbs in the treatment of neuropathic pain: a review, *Iranian Journal of Basic Medical Sciences* 21 (4) (2018) 347–358, <https://doi.org/10.22038/ijbms.2018.24026.6021>.
- [25] L. Yuan, X. Li, S. He, C. Gao, C. Wang, Y. Shao, Effects of natural flavonoid isorientin on growth performance and gut microbiota of mice, *J. Agric. Food Chem.* 66 (2018) 9777–9784, <https://doi.org/10.1021/acs.jafc.8b03568>.
- [26] K. Anilkumar, G.V. Reddy, R. Azad, N.S. Yarla, G. Dharmapuri, A. Srivastava, M.A. Kamal, R. Pallu, Evaluation of anti-inflammatory properties of isorientin isolated from tubers of, *Oxidative Med. Cell. Longev.* 2017 (2017) 5498054, <https://doi.org/10.1155/2017/5498054>.
- [27] L. Yuan, J. Wang, H. Xiao, W. Wu, Y. Wang, X. Liu, MAPK signaling pathways regulate mitochondrial-mediated apoptosis induced by isorientin in human hepatoblastoma cancer cells, *Food Chem. Toxicol.* 53 (2013) 62–68, <https://doi.org/10.1016/j.fct.2012.11.048>.
- [28] Qi-Yun Wu, Zack Chun-Fai Wong, Cheng Wang, Aster Hei-Yiu Fung, Emily Oi-Ying Wong, Gallant Kar-Lun Chan, Tina Ting-Xia Dong, Yicun Chen, Karl Wah-Keung Tsim, Isoorientin derived from *Gentiana veitchiorum* Hems. flowers inhibits melanogenesis by down-regulating MITF-induced tyrosinase expression, *Phytomedicine* 57 (2018) 129–136, <https://doi.org/10.1016/j.phymed.2018.12.006>.
- [29] Z. Zhang, Z. Liang, L. Yin, Q.X. Li, Z. Wu, Distribution of four bioactive flavonoids in maize tissues of five varieties and correlation with expression of the biosynthetic genes, *J. Agric. Food Chem.* 66 (2018) 10431–10437, <https://doi.org/10.1021/acs.jafc.8b03865>.
- [30] L. Yuan, S. Wei, J. Wang, X. Liu, Isoorientin induces apoptosis and autophagy simultaneously by reactive oxygen species (ROS)-related p53, PI3K/Akt, JNK, and p38 signaling pathways in HepG2 cancer cells, *J. Agric. Food Chem.* 62 (23) (2014) 5390–5400, <https://doi.org/10.1021/jf500903g>.
- [31] L. Yuan, Y. Wu, X. Ren, Q. Liu, J. Wang, X. Liu, Isoorientin attenuates lipopolysaccharide-induced pro-inflammatory responses through down-regulation of ROS-related MAPK/NF- $\kappa$ B signaling pathway in BV-2 microglia, *Mol. Cell. Biochem.* 386 (1–2) (2014) 153, <https://doi.org/10.1007/s11010-013-1854-9>.

- [32] Dehong Huang, Lei Jin, Zhengkang Li, Ji Wu, Ni Zhang, Dianrong Zhou, Xiaorong Ni, Teyong Hou, Isoorientin triggers apoptosis of hepatoblastoma by inducing DNA double-strand breaks and suppressing homologous recombination repair, *Biomed. Pharmacother.* 101 (2018) 719–728, <https://doi.org/10.1016/j.biopha.2018.02.142>.
- [33] X. Lin, Y. Chen, S. Lv, S. Tan, S. Zhang, R. Huang, L. Zhuo, S. Liang, Z. Lu, Q. Huang, *Glycyphila elegans* isoorientin attenuates CCL<sub>2</sub>-induced hepatic fibrosis in rats via modulation of NF- $\kappa$ B and TGF- $\beta$ 1/Smad signaling pathways, *Int. Immunopharmacol.* 28 (2015) 305–312, <https://doi.org/10.1016/j.intimp.2015.06.021>.
- [34] R. Narayanaswamy, A. Isha, L.K. Wai, I.S. Ismail, Molecular docking analysis of selected *Clinacanthus nutans* constituents as xanthine oxidase, nitric oxide synthase, human neutrophil elastase, matrix metalloproteinase 2, matrix metalloproteinase 9 and squalene synthase inhibitors, *Pharmacogn. Mag.* 12 (2016) S21–S26, <https://doi.org/10.4103/0973-1296.176111>.
- [35] Y. Tingting, S. Jiadong, H. Chaohao, Y. Dinglai, D. Shengjie, H. Xince, et al., Isoorientin induces apoptosis, decreases invasiveness, and downregulates VEGF secretion by activating AMPK signaling in pancreatic cancer cells, *OncoTargets and Therapy* 9 (2016) 7481–7492, <https://doi.org/10.2147/ott.s122653>.
- [36] K. Esra, A. Mustafa, G. İlhan, Y. Erdem, Evaluation of in vivo biological activity profile of isoorientin, *Z. Naturforsch., C, J. Biosci.* 59 (2004) 787–790.
- [37] J.D. Vry, E. Kuhl, P. Franken-Kunkel, G. Eckel, Pharmacological characterization of the chronic constriction injury model of neuropathic pain, *Eur. J. Pharmacol.* 491 (2–3) (2004) 137–148, <https://doi.org/10.1016/j.ejphar.2004.03.051>.
- [38] D.A. Dobecki, S.M. Schocket, M.S. Wallace, Update on pharmacotherapy guidelines for the treatment of neuropathic pain, *Curr. Pain Headache Rep.* 10 (2006) 185–190, <https://doi.org/10.1007/s11916-006-0044-9>.
- [39] C.C. Câmara, C.V. Araújo, K.K.O. de Sousa, G.A.C. Brito, M.L. Vale, R. da S. Raposo, F.E. Mendonça, B.S. Mietto, A.M.B. Martinez, R.B. Oriá, Gabapentin attenuates neuropathic pain and improves nerve myelination after chronic sciatic constriction in rats, *Neurosci. Lett.* 607 (2015) 52–58, <https://doi.org/10.1016/j.neulet.2015.09.021>.
- [40] G.J. Bennett, Y.K. Xie, A peripheral mononeuropathy in rat that produces disorders of pain sensation like those seen in man, *Pain* 33 (1) (1988) 87–107, [https://doi.org/10.1016/0304-3959\(88\)90209-6](https://doi.org/10.1016/0304-3959(88)90209-6).
- [41] S.R. Chaplan, F.W. Bach, J.W. Pogrel, J.M. Chung, T.L. Yaksh, Quantitative assessment of tactile allodynia in the rat paw, *J. Neurosci. Methods* 53 (1) (1994) 55–63, [https://doi.org/10.1016/0165-0270\(94\)90144-9](https://doi.org/10.1016/0165-0270(94)90144-9).
- [42] L. Jasmin, The cold plate as a test of nociceptive behaviors: description and application to the study of chronic neuropathic and inflammatory pain models, *Pain* 75 (2–3) (1998) 367, [https://doi.org/10.1016/S0304-3959\(98\)00017-7](https://doi.org/10.1016/S0304-3959(98)00017-7).
- [43] K. Hargreaves, A new and sensitive method for measuring thermal nociception in cutaneous hyperalgesia, *Pain* 32 (1988), [https://doi.org/10.1016/0304-3959\(88\)90026-7](https://doi.org/10.1016/0304-3959(88)90026-7).
- [44] E. Gabay, M. Tal, Pain behavior and nerve electrophysiology in the cci model of neuropathic pain, *Pain* 110 (1) (2004) 354–360, <https://doi.org/10.1016/j.pain.2004.04.021>.
- [45] S. Chiechio, A. Copani, R.W. Gereau, F. Nicoletti, Acetyl-L-carnitine in neuropathic pain: experimental data, *CNS Drugs* (2007) 31–38 null. discussion 45–6 <https://doi.org/10.2165/00023210-200721001-00005>.
- [46] N. Liu, Y.-X. Li, S.-S. Gong, J. Du, G. Liu, S.-J. Jin, C.-J. Zhao, Y. Niu, T. Sun, J.-Q. Yu, Antinociceptive effects of gentiopicroside on neuropathic pain induced by chronic constriction injury in mice: a behavioral and electrophysiological study, *Can. J. Physiol. Pharmacol.* 94 (2016) 769–778, <https://doi.org/10.1139/cjpp-2015-0462>.
- [47] M. Jarahi, V. Sheibani, H.A. Safakhah, H. Torkmandi, A. Rashidpour, Effects of progesterone on neuropathic pain responses in an experimental animal model for peripheral neuropathy in the rat: a behavioral and electrophysiological study, *Neuroscience* 256 (1) (2014) 403–411, <https://doi.org/10.1016/j.neuroscience.2013.10.043>.
- [48] Y. Sudoh, S.P. Desai, A.E. Haderer, S. Sudoh, P. Gerner, D.C. Anthony, U. De Girolami, G.K. Wang, Neurologic and histopathologic evaluation after high-volume intrathecal amitriptyline, *Reg. Anesth. Pain Med.* 29 (2004) 434–440, <https://doi.org/10.1097/00115550-200409000-00008>.
- [49] Baisong Zhao, Yongying Pan, Zixin Wang, Yonghong Tan, Xingrong Song, Intrathecal administration of tempol reduces chronic constriction injury-induced neuropathic pain in rats by increasing SOD activity and inhibiting NGF expression, *Cell. Mol. Neurobiol.* 36 (2016) 893–906, <https://doi.org/10.1007/s10571-015-0274-7>.
- [50] Meng-Ting Zhang, Bing Wang, Yi-Na Jia, Ning Liu, Peng-Sheng Ma, Shuai-Shuai Gong, Yang Niu, Tao Sun, Yu-Xiang Li, Jian-Qiang Yu, Neuroprotective effect of liquiritin against neuropathic pain induced by chronic constriction injury of the sciatic nerve in mice, *Biomed. Pharmacother.* 95 (2017) 186–198, <https://doi.org/10.1016/j.biopha.2017.07.167>.
- [51] H. Bostock, M. Campero, J. Serra, J.L. Ochoa, Temperature-dependent double spikes in C-nociceptors of neuropathic pain patients, *Brain* 128 (2005) 2154–2163, [https://doi.org/10.1016/S1474-4422\(10\)70143-5](https://doi.org/10.1016/S1474-4422(10)70143-5).
- [52] D.W.Y. Sah, M.H. Ossipo, F. Porreca, Neurotrophic factors as novel therapeutics for neuropathic pain, *Nat. Rev. Drug Discov.* 2 (2003) 460–472, <https://doi.org/10.1038/nrd1107>.
- [53] H. Koike, M. Iijima, K. Mori, M. Yamamoto, N. Hattori, H. Watanabe, F. Tanaka, M. Douy, G. Sobue, Neuropathic pain correlates with myelinated fibre loss and cytokine profile in POEMS syndrome, *J. Neurol. Neurosurg. Psychiatry* 79 (2008) 1171–1179, <https://doi.org/10.1136/jnnp.2007.135681>.
- [54] A.E. Valsecchi, S. Franchi, A.E. Panerai, P. Sacerdoti, A.E. Trovato, M. Colleoni, Genistein, a natural phytoestrogen from soy, relieves neuropathic pain following chronic constriction sciatic nerve injury in mice: anti-inflammatory and antioxidant activity, *J. Neurochem.* 107 (2008) 230–240, <https://doi.org/10.1111/j.1471-4159.2008.05614.x>.
- [55] Li Yuan, Jing Wang, Wanqiang Wu, Qian Liu, Xuebo Liu, Effect of isoorientin on intracellular antioxidant defence mechanisms in hepatoma and liver cell lines, *Biomed. Pharmacother.* 81 (2016) 356–362, <https://doi.org/10.1016/j.biopha.2016.04.025>.
- [56] L. Yuan, X. Han, W. Li, D. Ren, X. Yang, Isoorientin prevents hyperlipidemia and liver injury by regulating lipid metabolism, antioxidant capability, and inflammatory cytokine release in high-fructose-fed mice, *J. Agric. Food Chem.* 64 (2016) 2682–2689, <https://doi.org/10.1021/acs.jafc.6b00290>.
- [57] L.X. Wang, Z.J. Wang, Animal and cellular models of chronic pain, *Adv. Drug Deliv. Rev.* 55 (2003) 949–965, [https://doi.org/10.1016/s0169-409x\(03\)00098-x](https://doi.org/10.1016/s0169-409x(03)00098-x).
- [58] M. Sumizono, H. Sakakima, S. Otsuka, T. Terashi, K. Nakanishi, K. Ueda, S. Takada, K. Kikuchi, The effect of exercise frequency on neuropathic pain and pain-related cellular reactions in the spinal cord and midbrain in a rat sciatic nerve injury model, *J. Pain Res.* 11 (2018) 281–291, <https://doi.org/10.2147/JPR.S156326>.
- [59] A. Muthuraman, N. Singh, Neuroprotective effect of saponin rich extract of *Acorus calamus* L. in rat model of chronic constriction injury (CCI) of sciatic nerve-induced neuropathic pain, *J. Ethnopharmacol.* 142 (2012) 723–731, <https://doi.org/10.1016/j.jep.2012.05.049>.
- [60] D. Nuytten, R. Kupers, M. Lammens, R. Dom, J. Van Hees, J. Gybels, Further evidence for myelinated as well as unmyelinated fibre damage in a rat model of neuropathic pain, *Exp. Brain Res.* 91 (1992) 73–78, <https://doi.org/10.1007/bf00230014>.
- [61] C. Pan, C. Wang, L. Zhang, L. Song, Y. Chen, B. Liu, W.-T. Liu, L. Hu, Y. Pan, Procyanidins attenuate neuropathic pain by suppressing matrix metalloproteinase-9/2, *J. Neuroinflammation* 15 (2018) 187, <https://doi.org/10.1186/s12974-018-1182-9>.
- [62] L. Jiang, C.-L. Pan, C.-Y. Wang, B.-Q. Liu, Y. Han, L. Hu, L. Liu, Y. Yang, J.-W. Qu, W.-T. Liu, Selective suppression of the JNK-MMP2/9 signal pathway by tetra-methylpyrazine attenuates neuropathic pain in rats, *J. Neuroinflammation* 14 (2017) 174, <https://doi.org/10.1186/s12974-017-0947-x>.
- [63] S.R. Challa, Surgical animal models of neuropathic pain: pros and cons, *Int. J. Neurosci.* 125 (2015) 170–174, <https://doi.org/10.3109/00207454.2014.922559>.
- [64] N. Percie du Sert, A.S.C. Rice, Improving the translation of analgesic drugs to the clinic: animal models of neuropathic pain, *Br. J. Pharmacol.* 171 (2014) 2951–2963, <https://doi.org/10.1111/bph.12645>.
- [65] Jaggi Amteshwar Singh, Jain Vivek, Singh Nirmal, Animal models of neuropathic pain, *Fundam Clin Pharmacol* 25 (2011) 1–28, <https://doi.org/10.1111/j.1472-8206.2009.00801.x>.
- [66] R.L. Silva, A.H. Lopes, R.M. Guimarães, T.M. Cunha, CXCL1/CXCR2 signaling in pathological pain: role in peripheral and central sensitization, *Neurobiol. Dis.* 105 (2017) 109–116, <https://doi.org/10.1016/j.nbd.2017.06.001>.
- [67] C.J. Woolf, M.W. Salter, Neuronal plasticity: increasing the gain in pain, *Science* 288 (2000) 1765–1769, <https://doi.org/10.1126/science.288.5472.1765>.
- [68] M. Liu, K. Liao, C. Yu, X. Li, S. Liu, S. Yang, Puerarin alleviates neuropathic pain by inhibiting neuroinflammation in spinal cord, *Mediat. Inflamm.* 485927 (2014), <https://doi.org/10.1155/2014/485927>.
- [69] J.V. Berger, L. Knaepen, S.P.M. Janssen, R.J.P. Jaken, M.A.E. Marcus, E.A.J. Joosten, R. Deumens, Cellular and molecular insights into neuropathy-induced pain hypersensitivity for mechanism-based treatment approaches, *Brain Res. Rev.* 67 (2011) 282–310, <https://doi.org/10.1016/j.brainresrev.2011.03.003>.
- [70] R.-R. Ji, A. Nackley, Y. Huh, N. Terrando, W. Maixner, Neuroinflammation and central sensitization in chronic and widespread pain, *Anesthesiology* 129 (2018) 343–366, <https://doi.org/10.1097/ALN.0000000000002130>.
- [71] Jana Raputova, Iva Srotova, Eva Vlckova, Claudia Sommer, Nurcan Öveyler, Frank Birkelein, Heike L. Rittner, Cora Rebhorn, Blanka Adamova, Ivana Kovalova, Eva Kralickova Nekvapilova, Lucas Forer, Jana Belobradkova, Jindrich Olsovsky, Pavel Weber, Ladislav Dusek, Jiri Jarkovsky, Josef Bednarik, Sensory phenotype and risk factors for painful diabetic neuropathy: a cross-sectional observational study, *Pain* 158 (2017) 2340–2353, <https://doi.org/10.1097/j.pain.0000000000001034>.
- [72] A. Matsuoka, A. Mitsuma, O. Maeda, H. Kajiyama, H. Kiyoi, Y. Kodera, M. Nagino, H. Goto, Y. Ando, Quantitative assessment of chemotherapy-induced peripheral neurotoxicity using a point-of-care nerve conduction device, *Cancer Sci.* 107 (2016) 1453–1457, <https://doi.org/10.1111/cas.13010>.
- [73] A. Horst, J.A. de Souza, M.C.Q. Santos, A.P.K. Riffel, C. Kolberg, W.A. Partata, Effects of N-acetylcysteine on spinal cord oxidative stress biomarkers in rats with neuropathic pain, *Braz. J. Med. Biol. Res.* 50 (2017) e 6533, <https://doi.org/10.1590/1414-431X20176533>.
- [74] A.P.K. Riffel, J.A. de Souza, M. do C.Q. Santos, A. Horst, T. Scheid, C. Kolberg, A. Belló-Klein, W.A. Partata, Systemic administration of vitamins C and E attenuates nociception induced by chronic constriction injury of the sciatic nerve in rats, *Brain Res. Bull.* 121 (2016) 169–177, <https://doi.org/10.1016/j.brainresbull.2016.02.004>.
- [75] Y. Kawasaki, Z.-Z. Xu, X. Wang, J.Y. Park, Z.-Y. Zhuang, P.-H. Tan, Y.-J. Gao, K. Roy, G. Corfas, E.H. Lo, R.-R. Ji, Distinct roles of matrix metalloproteases in the early- and late-phase development of neuropathic pain, *Nat. Med.* 14 (2008) 331–336, <https://doi.org/10.1038/nm1723>.
- [76] V.N. Yong, Metalloproteinases: mediators of pathology and regeneration in the CNS, *Nat. Rev. Neurosci.* 6 (2005) 931–944, <https://doi.org/10.1038/nrn1807>.
- [77] W.-T. Liu, Y. Han, Y.-P. Liu, A. Song Angela, B. Barnes, X.-J. Song, Spinal matrix metalloproteinase-9 contributes to physical dependence on morphine in mice, *J. Neurosci.* 30 (2010) 7613–7623, <https://doi.org/10.1523/JNEUROSCI.1358-10.2010>.

- [78] A.K. Naik, S.K. Tandan, S.P. Dudhgaonkar, S.H. Jadhav, M. Kataria, V.R. Prakash, D. Kumar, Role of oxidative stress in pathophysiology of peripheral neuropathy and modulation by N-acetyl-L-cysteine in rats, *Eur. J. Pain* 10 (2006) 573–579, <https://doi.org/10.1016/j.ejpain.2005.08.006>.
- [79] Norimitsu Morioka, Keitaro Kodama, Mizuki Tomori, Kanade Yoshikawa, Munenori Saeki, Yoki Nakamura, Fang Fang Zhang, Kazue Hisaoka-Nakashima, Yoshihiro Nakata, Stimulation of nuclear receptor REV-ERBs suppresses production of pronociceptive molecules in cultured spinal astrocytes and ameliorates mechanical hypersensitivity of inflammatory and neuropathic pain of mice, *Brain Behav. Immun.* (2019), <https://doi.org/10.1016/j.bbi.2019.01.014> undefined, undefined.
- [80] Justin N. Siemian, Zach M. LaMacchia, Vilma Spreuer, Jingwei Tian, Tracey A. Ignatowski, Pablo M. Paez, Yanan Zhang, Jun-Xu Li, The imidazoline I receptor agonist 2-BFI attenuates hypersensitivity and spinal neuroinflammation in a rat model of neuropathic pain, *Biochem. Pharmacol.* 153 (2018) 260–268, <https://doi.org/10.1016/j.bcp.2018.01.032>.
- [81] A. Oprée, M. Kress, Involvement of the proinflammatory cytokines tumor necrosis factor- $\alpha$ , IL-1  $\beta$ , and IL-6 but not IL-8 in the development of heat hyperalgesia: effects on heat-evoked calcitonin gene-related peptide release from rat skin, *J. Neurosci.* 20 (2000) 6289–6293, <https://doi.org/10.1523/jneurosci.20-16-06289.2000>.
- [82] N.B. Finnerup, N. Attal, S. Haroutounian, E. McNicol, R. Baron, R.H. Dworkin, I. Gilron, M. Haanpää, P. Hansson, T.S. Jensen, P.R. Kamerman, K. Lund, A. Moore, S.N. Raja, A.S.C. Rice, M. Rowbotham, E. Sena, P. Siddall, B.H. Smith, M. Wallace, Pharmacotherapy for neuropathic pain in adults: a systematic review and meta-analysis, *Lancet Neurol.* 14 (2015) 162–173, [https://doi.org/10.1016/S1474-4422\(14\)70251-0](https://doi.org/10.1016/S1474-4422(14)70251-0).
- [83] A.M. Waszkielewicz, A. Gunia, K. Słoczyńska, H. Marona, Evaluation of anticonvulsants for possible use in neuropathic pain, *Curr. Med. Chem.* 18 (2011) 4344–4358, <https://doi.org/10.2174/092986711797200408>.
- [84] S. Derry, R.F. Bell, S. Straube, P.J. Wiffen, D. Aldington, R.A. Moore, Pregabalin for neuropathic pain in adults, *Cochrane Database Syst. Rev.* 1 (2019) CD007076, <https://doi.org/10.1002/14651858.CD007076.pub3>.
- [85] H. Dworkin Robert, B. O'Connor Alec, J. Audette, R. Baron, K. Gourlay Geoffrey, L. Haanpää Maija, L. Kent Joel, J. Krane Elliot, A. Lebel Alyssa, M. Levy Robert, C. Mackey Sean, J. Mayer, C. Miaskowski, N. Raja Srinivasa, S.C. Rice Andrew, E. Schmader Kenneth, B. Stacey, S. Stanos, R.-D. Treede, C. Turk Dennis, A. Walco Gary, D. Wells Christopher, Recommendations for the pharmacological management of neuropathic pain: an overview and literature update, *Mayo Clin. Proc.* 85 (2010) S3–14, <https://doi.org/10.4065/mcp.2009.0649>.
- [86] Gordon Munro, Inger Jansen-Olesen, Jes Olesen, Animal models of pain and migraine in drug discovery, *Drug Discov. Today* 22 (2017) 1103–1111, <https://doi.org/10.1016/j.drudis.2017.04.016>.
- [87] I.-C. Wang, C.-Y. Chung, F. Liao, C.-C. Chen, C.-H. Lee, Peripheral sensory neuron injury contributes to neuropathic pain in experimental autoimmune encephalomyelitis, *Sci. Rep.* 7 (2017) 42304, <https://doi.org/10.1038/srep42304>.
- [88] Danyal Daneshdoust, Mohsen Khalili-Fomeshi, Maryam Ghasemi-Kasman, Davoud Ghorbanian, Mona Hashemian, Mohammad Gholami, Aliakbar Moghadamnia, Amir Shojaei, Pregabalin enhances myelin repair and attenuates glial activation in lysolecithin-induced demyelination model of rat optic chiasm, *Neuroscience* 344 (2017) 148–156, <https://doi.org/10.1016/j.neuroscience.2016.12.037>.